

On the breakdown of ergodicity in a sheared foam

Yuhong Wang, Kapilanjan Krishan, and Michael Dennin

Department of Physics and Astronomy, University of California at Irvine, Irvine, California 92697-4575

(Dated: February 8, 2020)

A central tenant of statistical mechanics is the ergodic hypothesis: for sufficiently long times, a thermodynamic closed system may be expected to pass through almost all possible microstates [1]. If a system sufficiently explores phase space in this sense, then time averages of physical quantities are equivalent to ensemble averages [2, 3, 4, 5]. This result is incredibly powerful, and an important issue is the degree to which this concept can be expanded to driven systems, especially ones on the mesoscopic scale. Such systems include fluids confined in micro- or nano-fluidic devices, materials with high binding energies (mesoscopic clusters, nano-droplets), and complex fluids composed of macroscopic particles (granular matter, emulsions, foams). Especially for complex fluids, there is a significant interest in the behavior of the velocity profiles due to measurements of interesting nonlinear behavior [6, 7, 8, 9, 10, 11]. Understanding this behavior requires comparison of theoretical studies of the source and the stability of such velocity profiles [12, 13, 14, 15, 16] with the experimental results. Such comparisons depend critically on an understanding of the averaging process. Here we directly compare time and ensemble averages for velocity profiles in a bubble raft. The long time-averaged velocity profiles converge in a well-defined manner. However, long-time averages of individual members of the ensemble are found to be measurably different from the ensemble average. In addition to the impact on our understanding of flow in complex fluids, this demonstrates a difference between fluctuations induced by flow and thermal fluctuations in the context of how systems explore phase space. Understanding these differences has an impact on the further development of the theoretical framework underlying the proposed jamming paradigm [17] and other proposals for understanding driven systems based on the nature of their fluctuations[18].

The connection between flow induced fluctuations and thermal fluctuations is worth further comment. A bubble raft consists of bubbles floating on the surface of water [11, 19]. Compared to the strong interactions between bubbles, thermal fluctuations play no significant role in the dynamics of the flow. This is a common situation in mesoscopic flows where the particles are often sufficiently large that thermal fluctuations are not relevant and in which fluctuations induced by the driving force play a critical role (see for example, [20]). Various sce-

narios connecting flow induced fluctuations with thermal fluctuations are receiving significant attention, including ideas of jamming phase diagrams [17, 21] and effective temperatures [22, 23, 24]. Our comparisons of time and ensemble averages provide a test of the connection between flow induced and thermal fluctuations and suggest fundamental limits on this connection.

The flow induced fluctuations are a result of the local kinematics of the bubbles in response to the applied rate of strain [25]. The initial response of the bubbles is to deform elastically. If the local stress is sufficiently high, bubbles undergo nonlinear rearrangements. These are referred to as T1 events. Two bubbles that are originally nearest neighbors become next nearest neighbors. At the same time, two different bubbles that are next nearest neighbors become neighbors. These are the fundamental nonlinear events that generate flow. Finally, there are collective motions involving many T1 events with large regions of bubble rearrangement. These large scale events can be related to sudden changes of the macroscopic stress stored in the system [26]. As a result of these collective motions, topological variations associated with individual T1 events are transported through the system. These fundamental bubble motions are illustrated in Fig. 1. By generating fluctuations in the velocity due to rapid changes in the positions of the bubbles, it is these nonlinear transitions that may drive ergodic dynamics when the system is subjected to continual strain.

The bubble raft is produced by flowing regulated nitrogen gas through a needle into a homogeneous solution of 80% by volume deionized water, 15% by volume glycerine, and 5% by volume Miracle Bubbles (from Imperial Toy Corporation). The bubbles are confined between two parallel bands separated by a distance D . The bands are driven at a constant velocity v_w in opposing directions. This applies a steady rate of strain to the system given by $\dot{\gamma} = 2v_b/d$. The total applied strain is $\gamma = \dot{\gamma}t$, where t is the time interval under consideration. The direction of flow imposed by the bands is taken to be parallel to the x-axis. By tracking the individual motions of the bubbles, we compute the average velocity profile $\langle v_x(y) \rangle_\gamma$, where the y direction is taken perpendicular to the bands and $\langle \rangle_\gamma$ indicates that the average is over a particular strain interval. (Because the experiments are at a constant rate of strain, averages over time and strain differ by only a scalar constant of proportionality.) Here $v_x(y)$ represents an average over all bubbles in a bin of width dy at a distance y from the center between the bands and extended along the x-axis. Unless stated, plots are of the normalized x-component of the velocity (v_x/v_w) as a function of the position normalized by the bubble

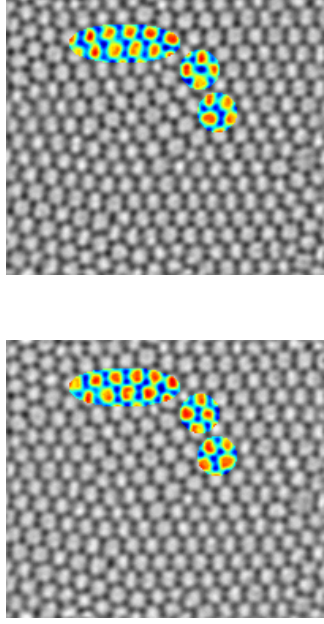


FIG. 1: A typical set of consecutive images representing the instantaneous structure of the bubble raft. Shear induced through the bands on the top and bottom cause the material to yield through slip between neighboring bubbles (T1 events). These local events (highlighted) cause fluctuations in the velocity profiles of the bubbles, that average out over long times.

diameter (y/D). Details of the apparatus and methods can be found in Ref. [27].

Before comparing time and ensemble averages, it is necessary to establish the convergence of time averages, consistent with a stationary distribution of states during evolution. In addition, the convergence of the time averages provides its own probe of the nature of the athermal fluctuations. The importance of understanding the time average itself is highlighted by work in granular matter in which extremely long times were required for convergence of the average density under tapping [20]. Figure 2a illustrates typical velocity profiles that are achieved by averaging over a strain interval of 0.1 taken at different points in a run to total strain 5. A straight line is included as a guide to the eye. This demonstrates the fluctuating nature of short time velocity profiles. By considering the behavior at different times in the run, we establish the persistence of the fluctuations throughout the entire time during which the flow is imposed on the system. A striking feature of the profiles is the fact that they do not reflect the symmetry of the applied rate of strain. For any given strain interval, we observe profiles that fluctuate above and below the expected straight line behavior, as well as ones that are either consistently above or consistently below this line.

As one increases the strain interval used to compute

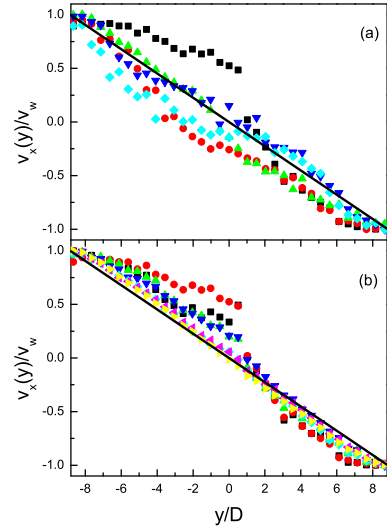


FIG. 2: The different curves in the upper figure are velocities of the bubbles as a function of the position across the trough that are computed over a strain interval of 0.1 taken at different times in the total run. The large fluctuations are induced due to local reorganization of the foam through T1 events. These fluctuations are indicative of the inherent non-newtonian behavior of the material. The lower figure indicates the convergence of the velocity profiles through averaging over increasing amount of time (or strain). The colors represent increasing intervals of strain in the following order: black, red, blue, light blue, purple, yellow.

the averages, the average velocity approaches a linear profile more closely, as indicated in Fig. 2b. Scaling the velocity components by the velocity of the bands, results in velocity profiles that coincide. This implies a scale independence for the long time average velocities in the system. This fact motivates the consideration of averages in terms of strain instead of time, for direct comparison between different applied rates of strain.

To quantify the convergence and the rate of convergence, we measured two different quantities: $\delta v_L(\gamma)$ and $\delta v_f(\gamma)$. Essentially, $\delta v_L(\gamma)$ measures the deviation of a short-time average from a linear profile and $\delta v_f(\gamma)$ measures the deviation of a short-time average from the average over the total strain of 5. More specifically, $\delta v_L(\gamma) = \sqrt{<(v - \bar{v}_L)^2>_\gamma}$ and $\delta v_f(\gamma) = \sqrt{<(v - \bar{v}_f)^2>_\gamma}$, where v is the instantaneous x-component of the velocity, \bar{v}_L or \bar{v}_f denotes a linear velocity profile or the average of instantaneous velocities over the total strain applied, respectively. The braces, $<>_\gamma$, refer to an average over all bubbles being considered, and over a strain γ . Figure 3 indicates the value of $\delta v_f(\gamma)$ as a function of the total external strain applied to the bubble raft, and the insert in Fig. 3 is a plot of $\delta v_L(\gamma)$. The different curves are for different rates of strain. The fact that they essentially collapse reflects the independence of the behavior on the

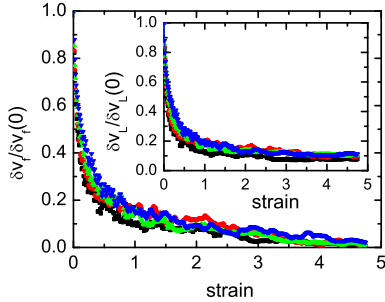


FIG. 3: The measure of the convergence of the velocity profiles relative to the final average profile ($\delta v_f(\gamma)/\delta v_f(0)$) versus strain for different rates of strain. The convergence factors have been scaled by the value at a strain of zero for direct comparison between different rates of strain. For comparison, the insert is a plot of the convergence with respect to a linear profile ($\delta v_L(\gamma)/\delta v_L(0)$) for the same experimental runs. The main difference between the two measures is the offset that exists for $\delta v_L(\gamma)/\delta v_L(0)$.

rate of strain. The most striking features are that (a) the profiles converge in a well-defined manner and (b) there is a measurable difference between the final velocity profile and a linear profile.

These last two statements relate to the functional form of $\delta v_L(\gamma)$ and $\delta v_f(\gamma)$. Both sets of data are well fit by a double exponential. The difference being that $\delta v_f(\gamma)$ is well fit with zero offset, establishing that the system is converging to a well-defined final state. However, fits of $\delta v_L(\gamma)$ consistently require a non-zero offset (on the order of 0.1 for all rates of strain), indicating a measurable difference between the final converged state and a linear profile. The fit to a double exponential suggests that at least two dominant strain scales govern the convergence to the final profile. It is not possible to obtain a good fit with a single exponential. Referring back to the qualitative behavior indicated in Fig. 1, one can associate the shorter strain scale with the individual T1 events and the longer scale with the large collective motions. Further work will be needed to make this statement precise.

Given that the time averages are well-defined, we can compare them with an ensemble average. The primary distinction between the different members of the ensemble are in the initial spatial distributions of the bubbles. A true ensemble average would average over all allowed microstates. To approximate an ensemble average, we average the time-averaged velocity profiles for a series of different initial conditions. As each initial state results in different time-averages, these represent different explorations of the allowed microstates, and averaging over results for different initial conditions approximates an ensemble average. Because we have already shown that all of the behavior is independent of rate of strain, we will focus on five different realizations of a bubble raft and determine the velocity profile for each realization using

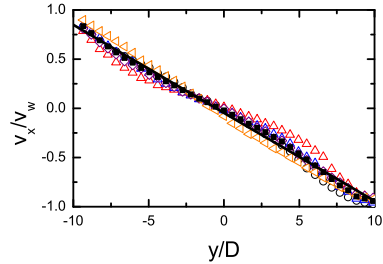


FIG. 4: Velocity profiles for different realizations of a bubble raft (open symbols) as a function of the position perpendicular to the walls (error in the velocity measurement is equal to or smaller than the symbol size). For comparison, the ensemble average of the five runs (solid squares) and a linear profile (line) are shown.

an applied rate of strain of 0.014 s^{-1} . Figure 4 is a plot of the 5 different velocity profiles and their average. Each profile represents a strain-averaged profile over a strain of 5. As expected, the differences between the individual profiles are on the same order as their differences from a linear profile (as measured by δv). Therefore, each realization of the bubble raft results in a different time-averaged velocity profile. Comparing the ensemble averaged profile (for only 5 runs) and a linear profile gives $\delta v_L = 0.03 \text{ mm/s}$. For comparison, the typical difference between a time averaged result and the linear profile for the same rate of strain is $\delta v_L = 0.14 \text{ mm/s}$. (The difference between different time averaged profiles is also on the order of $\delta v = 0.14 \text{ mm/s}$.) This establishes two things: (1) the ensemble average and time average are measurably different and (2) the ensemble average converges to a linear profile.

These experiments show that the fluctuations during flow produce well-defined time-averaged velocity profiles that are nonlinear. Furthermore, the final state of the system depends strongly on the initial bubble configuration. Presumably this is due to the fact that the fluctuations during flow do not provide sufficient exploration of phase space to produce time-average velocity profiles that are independent of initial conditions. Finally, after ensemble averaging linear profiles emerge. The time average does not equal the ensemble average.

These experiments focus on the athermal nature of fluctuations in a flowing foam as the source of the difference between time and ensemble averages. Previous studies with bubble rafts indicate that the nature of the fluctuations is independent of system size, even for these relatively small systems [28], suggesting system size is not critical. However, as the issue of average behavior explicitly probes the ability of the system to explore state space, the impact of system size needs to be explored in more detail in regards to this particular problem. The results underline the need to distinguish thermal and athermal fluctuations, particularly when studying the evolu-

tion of mesoscopic systems. Will a sufficiently small thermal system exhibit similar behavior, or is it the fundamental feature of these systems that produces these results the nature of the fluctuations? This is a question that can be explored in simulations, and may have an important impact on various nano-fluidic applications.

Acknowledgments

This work was supported by Department of Energy grant DE-FG02-03ED46071. The authors thank Corey O'Hern and Manu for useful discussions.

[1] L. Boltzmann, *Wiener Berichte* **63**, 712 (1871).

[2] L. Boltzmann, *Nature* **51**, 413 (1895).

[3] L. Boltzmann, *Nature* **52**, 221 (1895).

[4] L. D. Landau and E. M. Lifshitz, *Statistical Physics (Third Edition), Part 1* (Butterworth-Heinemann, Oxford, 1980).

[5] R. K. Pathria, *Statistical Mechanics(Second Edition)* (Butterworth-Heinemann, Oxford, 1996).

[6] D. M. Mueth, G. F. Debregeas, G. S. Karczmar, P. J. Eng, S. R. Nagel, and H. M. Jaeger, *Nature* **406**, 385 (2000).

[7] W. Losert, L. Bocquet, T. C. Lubensky, and J. P. Gollub, *Phys. Rev. Lett.* **85**, 1428 (2000).

[8] D. Howell, R. P. Behringer, and C. Veje, *Phys. Rev. Lett.* **82**, 5241 (1999).

[9] P. Coussot, J. S. Raynaud, F. Bertrand, P. Moucheront, J. P. Guilbaud, H. T. Huynh, S. Jarny, and D. Lesueur, *Phys. Rev. Lett.* **88**, 218301 (2002).

[10] J.-B. Salmon, A. Colin, S. Manneville, and F. Molino, *Phys. Rev. Lett.* **90**, 228303 (2003).

[11] J. Lauridsen, G. Chanan, and M. Dennin, *Phys. Rev. Lett.* **93**, 018303 (2004).

[12] P. A. Thompson and G. S. Grest, *Phys. Rev. Lett.* **67**, 1751 (1991).

[13] S. Y. Liem, D. Brown, and J. H. R. Clarke, *Phys. Rev. A* **45**, 3706 (1992).

[14] F. Varnik, L. Bocquet, J.-L. Barrat, and L. Berthier, *Phys. Rev. Lett.* **90**, 095702 (2003).

[15] N. Xu, C. S. O'Hern, and L. Kondic, *Phys. Rev. Lett.* **94**, 016001 (2005).

[16] N. Xu, C. S. O'Hern, and L. Kondic, *cond-mat* p. 0506507 (2005).

[17] A. J. Liu and S. R. Nagel, *Nature* **396**, 21 (1998).

[18] D. J. Pine, J. P. Gollub, J. F. Brady, and A. M. Leshansky, *Nature* **438**, 997 (2005).

[19] L. Bragg and W. M. Lomer, *Proc. R. Soc. London, Ser. A* **196**, 171 (1949).

[20] E. R. Nowak, J. B. Knight, E. Ben-Naim, H. M. Jaeger, and S. R. Nagel, *Phys. Rev. E* **57**, 1971 (1998).

[21] A. J. Liu and S. R. Nagel, eds., *Jamming and Rheology* (Taylor and Francis Group, 2001).

[22] L. F. Cugliandolo, J. Kurchan, and L. Peliti, *Phys. Rev. E* **55**, 3898 (1997).

[23] I. K. Ono, C. S. O'Hern, D. J. Durian, S. A. Langer, A. J. Liu, and S. R. Nagel, *Phys. Rev. Lett.* **89**, 095703 (2002).

[24] L. Berthier and J.-L. Barrat, *Phys. Rev. Lett.* **89**, 095702 (2002).

[25] D. Weaire and S. Hutzler, *The Physics of Foams* (Clarendon Press, Oxford, 1999).

[26] M. Dennin, *Phys. Rev. E* **70**, 041406 (2004).

[27] Y. Wang, K. Krishan, and M. Dennin, *Phys. Rev. E* **73**, 031401 (2006).

[28] E. Pratt and M. Dennin, *Phys. Rev. E* **67**, 051402 (2003).